

A Computational Model of Afterimages

Tobias Ritschel^{1,2} Elmar Eisemann¹

¹Télécom ParisTech (CNRS-LTCI) ²Intel Visual Computing Institute



Figure 1: Afterimage simulation of a traffic light over time. Note the over-time change of colors, blur and shape in the afterimage.

Abstract

Afterimages are optical illusions, particularly well perceived when fixating an image for an extended period of time and then looking at a neutral background, where an inverted copy of the original stimulus appears. The full mechanism that produces the perceived specific colors and shapes is complex and not entirely understood, but most of the important attributes can be well explained by bleaching of retinal photoreceptors (retinal kinetics). We propose a model to compute afterimages that allows us to simulate their temporal, color and time-frequency behavior. Using this model, high dynamic range (HDR) content can be processed to add realistic afterimages to low dynamic range (LDR) media. Hereby, our approach helps in conveying the original source's luminance and contrast. It can be applied in real-time on full-HD HDR content using standard graphics hardware. Finally, our approach is validated in a perceptual study.

Categories and Subject Descriptors (according to ACM CCS): I.3.7 [Computer Graphics]: Three-Dimensional Graphics and Realism—Color, shading, shadowing, and texture

1. Introduction

For (chromatic) adaptation our visual system reacts to the perceived radiance and influences our perception of the scene. While this process is naturally employed by our Human Visual System (HVS) in the real-world, it is necessary to simulate such behavior when depicting virtual scenes. Many modern games and simulations rely on simple models and tone corrections to achieve a similar experience, which is important for a realistic look.

While previous approaches considered global manipulations (such as gamma curves), our model goes further. We consider afterimages. This fatigue-like effect results in an antagonistic color perception which becomes especially visi-

ble when fixating on a monochrome wall after observing a bright colorful object. The main mechanism behind this process is the bleaching of retinal photoreceptors. In computer graphics, bleaching has previously received attention in the context of tone mapping and color appearance modeling, but, in this paper, we propose a new model to compute afterimages based on a localized process that considers temporal, color and time-frequency behavior (e. g., blurred fading over time under varying colors).

Our method results in increased realism concerning the depiction of perceived strong luminance, and can be used to convey HDR content on an LDR medium. While afterimages arise in the observer's eye while looking at an LCD, the brightness of standard screens is insufficient to produce

correct afterimages with respect to HDR-image content. Our model can be used to correct this shortcoming and even leads to an increase in perceived brightness. We achieve real-time rates for full-HD content and illustrate the effectiveness of our method in a perceptual study.

This paper is structured as follows. After discussing previous work (Sec. 2), we introduce our approach (Sec. 3) and present results (Sec. 4), before concluding (Sec. 5).

2. Related Work

In this section, we will discuss related work, both from computer graphics, as well as general vision and physiology.

Afterimages Most features of afterimages are explained by the adaptation [Alp71] of the human retina's photo-receptor cells [Bri62]: its *receptor kinetics*. A receptor is a cell that transforms light in form of photon energy into an electric signal. This energy transformation happens due to a class of proteins called *opsins*. The chemical processes behind transduction of light to impulses (their kinetics) is complex, but can be predicted using a cascade of coupled equations e. g., for turtles [BHL74].

Photoreceptor kinetics, in its most simple form, describes the change of opsin concentration over time (Fig. 2) using two basic principles. First, when a receptor is exposed to light, a signal is triggered and the opsin concentration is lowered. The lower the opsin concentration, the less responsive the receptor. Conceptually, opsin flowing out of the receptor leads to a *deactivation*. When the opsin concentration is zero, the receptor *saturates*. Nonetheless, opsin is constantly regenerated from deactivated opsin; hereby *reactivating* the receptor. This process explains the basic principle of afterimages well. They occur when the receptor cell cannot adapt quickly enough to react to illumination changes.

The receptor signals are believed to be combined into the perception of color by opponent processes. When a receptor becomes adapted, the opposite color appears [Loo72]. This agrees with the percept of afterimages, e. g., a green stimulus produces a red afterimage, etc [ARH78]. Further evidence for a retinal explanation is the fact that the presence of glare does not trigger any strengthening of afterimages [LZL06].

Under normal viewing conditions, the receptor rarely saturates. One reason are saccades [MCMH04]: a moving eye receives constantly changing light on the retina. Even when fixating a natural stimulus, microsaccades happen and depending on the constant areas in the stimulus, differently sized areas of adaptation occur, as well as blur that becomes visible in resulting afterimages.

The human retina consists of two types of photoreceptors: cones and rods. Most of the afterimages can be attributed to cones that are active in photopic (daylight) vision and respond to different wavelengths in different ways. Rods

are mostly used in dark vision and saturated in photopic conditions. As these conditions are mostly of interest to us, we will concentrate on cones. Nonetheless, one should point out that the perception of afterimages is different between photopic and scotopic conditions [Ade82, HHDH09], but the kinetics can be similarly described.

There are three types of cones, L, M and S cones, each with a spectral response roughly equivalent to red (long), green (medium) and blue (short) wavelengths. Cones are densely packed in the fovea and more sparse in the periphery.

Besides colors, a distinct property of afterimages is their increased blurring over time. Creed [Cre28] studied the effect using sinusoidal gratings of different colors, orientation and frequency as stimuli, resulting in quantitative measurements of blur used in this work.

As mentioned, the full explanation of afterimages is not purely retinal nor purely cortical [Lan64], but as for chromatic and luminance adaptation a strong relation to receptor kinetics [Rus65] exists and will be the basis of our model. Other forms of afterimages (presumably cortical; not considered in this article) are perceived when quickly altering patterns of light elicit colors [VL77], or for filled-in surfaces [SKN01]. Here, a retinal-only explanation would be insufficient.

Computer graphics After the first models of photoreceptor kinetics became available [BHL74], hardware to simulate a single receptor was designed [VCP80], but did not aim at image synthesis.

Color-appearance models account for adaptation [Fai05]. Their extension to image appearance, such as iCAM [FJ04, KJF07], considers spatial locality. In all such models, adaptation is time-stationary, i. e., its change is not considered. Instead, our model predicts how a certain stimulus at a point in time is perceived given previous stimuli over time.

Classic computer-graphics models of the HVS's adaptation were introduced by Pattanaik et al. [PFFG98, PTYG00] in the context of tone mapping. They model the global adaptation to different lighting conditions in terms of thresholds, but not its localized retinal effect that results in afterimages. In [GAMS05] a model for pigment bleaching in the human retina including the Stiles-Crawford effect [SC33] is presented. We extend upon this model, by considering localized photoreceptor kinetics and the temporal behavior of afterimage color and sharpness. Adaptation and bleaching is routinely simulated using time-varying, global tone adjustments in interactive applications such as computer games.

Recently, Pajak et al. [PCA*10] proposed a computational model of lightness maladaptation. This model indeed accounts for the local response of the HVS to high contrast. However, their model does not account for afterimages, their color, or fading, and only considers threshold elevation.

3. Our approach

This section explains our model of afterimages and its efficient implementation for real-time performance. Our approach gives rise to several applications that will be presented in Sec. 4 together with a perceptual study.

3.1. Model

The different stages of our model are depicted in Fig. 2. We assume photopic conditions, i. e., daylight with color vision dominated by cones, and exclude rods from our simulation. We consider several processes that are involved in the perception of afterimages. First, world radiance is converted into an eye radiance map taking subconscious micro eye movement into account. On the retina, receptor kinetics are used to derive the perceived afterimage stimulus. The simulation includes a model of adaptation state, temporal diffusion, and chromatic influence. The result is combined with the input to derive the complete stimulus.

World radiance Input to our model is an HDR *world*-radiance map $L_w(\mathbf{x}, \lambda)$, i. e., the display content at position \mathbf{x} for wavelength λ . We assume a virtual (i. e., “cyclopean”) eye, looking forward without saccadic movements. The average over the frame interval s is denoted as L_w .

Eye radiance and Dynamics To simulate an eye-internal phenomenon such as afterimages, an *eye* radiance map $L_e(\mathbf{x}, \lambda)$ is produced. It encodes the radiance arriving at \mathbf{x} after compensating for the eye’s dynamics. To account for eye dynamics we rely on a fixation function $f: \mathbb{R}^2 \times \mathbb{R} \rightarrow \mathbb{R}^2$ that maps a location \mathbf{x} at a point in time t to another location $f(\mathbf{x}, t)$. The eye radiance according to this model is then

$$L_e(\mathbf{x}, \lambda) = \int_0^s L_w(f(\mathbf{x}, t), \lambda) dt. \quad (1)$$

Eye tracking equipment is the optimal solution to acquire f . In the absence of eye tracking, a simple assumption is that the observer fixates the screen center, i. e., $f(\mathbf{x}, t) = \mathbf{x}$, which is a common assumption for image-appearance modeling [Fai05]. While this scenario eliminates strong eye movement, small dynamics can still have an important impact on afterimages and need to be considered.

A fixation f that models small-scale dynamics well [MCMH04] uses a three-component saccade model: Saccades (mag. ≈ 10 cyc/deg, freq. ≈ 3 Hz), micro-saccades (mag. 0.1 cyc/deg, freq. ≈ 100 Hz) and tremor (mag. 0.01 cyc/deg, freq. ≈ 1 kHz). A typical frame time is $s \approx 32$ ms for a 30 Hz display. As saccades are proportionally rare compared to s and tremor is weak compared to the screen resolution both can be neglected. However, micro-saccades do have an effect as they occur during s and are larger than pixels. Micro-saccades are small random movements that follow a Gaussian distribution [MCMH04]. Consequently, the temporal impact of a static world radiance in Eq. 1 can be modeled well with a spatial convolution using a Gaussian kernel.

A viewing distance of ≈ 1 m results in a blur kernel of ≈ 10 px for a 1280×1024 screen [MCMH04]. Hereby, we can avoid eye tracking by assuming a static eye and a blurred stimulus, instead of a dynamic eye and a static stimulus.

Retinal and effective radiance The eye radiance map $L_e(\mathbf{x}, \lambda)$ is converted into *retinal* radiance (Trolands) by accounting for the pupil radius in the same way as [GAMS05]. The different sensitivity for different directions (Stiles-Crawford effect) is taken into account by a spatially varying efficiency ratio map. The resulting quantity is called the *effective* radiance $L(\mathbf{x}, \lambda)$. Finally, spectral effective radiance is converted into an LMS color space representation $L(\mathbf{x})$ using the standard observer LMS profiles. Next, the retinal kinetics of every photoreceptor are simulated.

Retinal kinetics While Baylor [BHL74] identified a cascade of up to six different chemicals that would need to be modeled, we found a simplified model of a single chemical sufficient for a qualitative effect. Note that both Baylor’s six and our single chemical are “virtual” in the sense that it cannot be concluded that exactly six individual chemicals are involved in reality. Instead, they should be interpreted as more or less accurate parameters fitted to data (physiological measurements in turtles for Baylor; functionally plausible images for our purpose). Nonetheless, a more complex multi-chemical model could be used.

Formally, consider the time-space varying ratio of active opsin left in a unit area covered by L, M and S cones:

$$r_{\{L,M,S\}}: \mathbb{R}^2 \times \mathbb{R} \rightarrow [0, 1]. \quad (2)$$

Furthermore, every receptor’s time-space varying change of active opsin over time at position \mathbf{x} and time t is $\dot{r}(\mathbf{x}, t)_{\{L,M,S\}}$. In the following, we drop the LMS index and treat r and \dot{r} as 3-vectors. The change of opsin concentration depends on the effective radiance and the current adaptation [BHL74], following the equation:

$$\dot{r}(\mathbf{x}, t) = c_a L(\mathbf{x}, t)(1 - r(\mathbf{x}, t)) - c_d r(\mathbf{x}, t), \quad (3)$$

where c_a resp. c_d are constants of activation and deactivation.

Eq. 3 shows that opsin concentration r follows two mechanisms that are balanced off by the concentration itself. When a receptor is exposed to strong effective radiance or is not yet strongly adapted (r is small), the change of adaptation is faster, i. e., it activates faster. For a progressed adaptation the activation is reduced (towards $r = 1.0$). A similar behavior occurs if the effective radiance is low. Interestingly, the opsin deactivation is independent of the effective radiance, but inversely proportional to the current bleaching. Hence, the deactivation is slow when little adaptation has happened, and fast, when much opsin was activated. Choosing $c_a = 0.3$ and $c_d = 1.0c_a$ gave good results for our one-chemical model - an average over three test subjects that were asked to adjust the parameters.

A Newton solver numerically integrates the differential

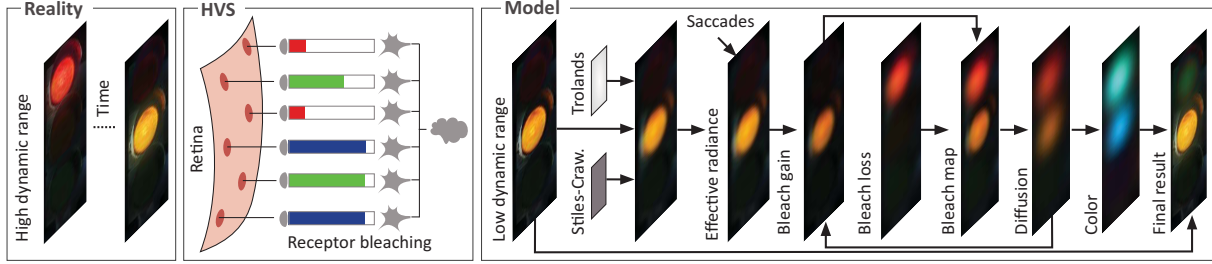


Figure 2: A stimulus can result in afterimages produced by the HVS, which are simulated by our model. The stimulus (left) is a time-varying HDR radiance map, here, a traffic light. In the HVS (middle), photoreceptors (red circles) of different types (long, middle and short wavelength) cover the retina (surface). The pigment concentration in each receptor is depicted by bars, resulting in differing color perception. In our model, different steps (right box) simulate receptor kinetics computationally.

Eq. 3 forward in time. In each step, the solution is clamped to $[0, 1]$. The adaptation change \dot{r} is maximal for $r = 0$ and proportional in change to L/n . Hence, a single iteration ($n = 1$) is usually sufficient given our framerates and changes in L .

Diffusion As noted in [Cre28], afterimages undergo considerable progressive blurring over time. While the underlying principles of this phenomenon are not fully understood, we can simulate its behavior. The time-frequency nature has been measured (Fig. 3 in [Bri62]) and enables us to fit a corresponding smoothing process according to these curves. When f frames are shown per second, the Gaussian kernel \mathcal{N}_σ needs to be chosen $\sigma = \mathcal{N}_\sigma / \sqrt{f}$ to obtain correct blur level, as indicated in [Bri62], after one second. Note, that the diffusion blur is not related to the blur due to saccadic eye movements, which is applied to the input only once.

Chromatic effect The bleaching result cannot be simply subtracted from the effective radiance in LMS color space and converted back to RGB for display, as the HVS employs an opponent color processing that we need to account for. Red stimuli lead to green afterimages, orange stimuli to blue afterimages, etc. To this end, we transform the bleaching from LMS into an opponent color space (we use oRGB [BBS09], which is a linear transform that was conceived according to the mechanism). We compute the opponent color of the current bleaching, transform it back to RGB and compose with the LDR input for final display.

3.2. LDR Compensation

When depicting HDR content on an LDR medium, the resulting real afterimage is different, i. e., weaker than it would be had the observer looked at HDR content. To produce a percept closer to the one resulting from the original HDR content, we can use our model to compute the afterimage that the HDR content would have produced, and insert it into the LDR image. If required, we can compensate for the weak afterimage produced by the LDR content in the observer's eye following the same model, but, in practice, the real LDR afterimage is weak enough to be neglected.

```

for  $i = 1 \dots n$ 
  for each  $r_j$  in  $\mathcal{R}$  parallel
     $\dot{r}_j \leftarrow c_a \mathcal{L}_j (1 - r_j) - c_d r_j$ 
     $r_j \leftarrow r_j + \frac{s}{n} \dot{r}_j$ 
  for each  $r_j$  in  $\mathcal{R}$  parallel
     $r_j \leftarrow \text{convolve}(\mathcal{R}, \mathcal{N}_\sigma)_j$ 

```

Listing 1: Pseudocode for one simulation step: n is the number of Newton iterations, \mathcal{R} the receptors, \mathcal{L} the effective radiance, s the time step and $c_{\{d,a\}}$ the (de-)activation ratio.

3.3. Flight of colors

A final component of afterimages is the so-called “flight of colors”: afterimages that change their hue continuously over time. In practice, this effect is usually only observed when closing the eyes or when suddenly being in a very dark environment. There is no physiological data available concerning this process – and maybe there never will be; the effect is subjective and it seems almost a philosophical question approaching the limits of human introspection. Shuey [Shu24] collected sample sequences of various researchers and philosophers. We can optionally simulate flight of color by applying a hue rotation in every simulation step.

3.4. Implementation

We rely on an Nvidia GeForce 480 GTX to execute our model for m receptors in parallel (cf. Listing. 1) using OpenGL. We assume one receptor for every pixel, ignoring their, in reality, more complex spatial layout and varying density [Dee05]. Input to our model is the effective radiance as a GPU vector \mathcal{L} of size m and the time step s . The current adaptation of every receptor is stored in a GPU vector \mathcal{R} , also of size m . All m threads compute a new adaptation state, from the current effective radiance and the previous adaptation state according to Eq. 3, integrating it forward in time in n steps per frame. Using 16 bit floating point-precision, the resulting kernel can process 300Mpixel/s with a single iteration. For a multi-chemical model, each stage requires one GPU buffer.

4. Result

We present two main results: example applications (prediction, tone mapping, and improved brightness appearance) of our model and a study showing its validity and effectiveness.

4.1. Applications

We present three prototypic scenarios and applications for our model that are also illustrated in the accompanying video.

Simulation scenario Our model allows us to predict visibility in different viewing conditions, which can be critical for many applications, e. g., training software for cars, ships or airplanes. As an example, we simulate the effects of afterimages on a traffic light under difficult, high-contrast conditions (Fig. 1 and Fig. 3, middle).

HDR photo viewer scenario Depicting high-contrast content as found in many HDR (panorama) images is challenging. To produce a percept closer to the one resulting from the original HDR content, we use our model to compute an afterimage that the HDR content would have produced, and insert it into the LDR image. This is similar to the popular introduction of glare around bright light sources in interactive applications such as computer games. We apply our approach to a panoramic HDR image viewer (Fig. 3 top).

Game scenario Our solution can increase the perceived brightness of explosions, fire and bright light. Further, in a game, our assumptions (changing content, fixation on screen center) are more likely to hold. In Fig. 3, bottom, both afterimages are due to bright daylight shafts in a dark room.

4.2. Perceptual study

Two perceptual studies verify that our approach is able to present HDR content on an LDR screen such that it is perceived brighter. We used a Samsung RZ 2233 display (1680 × 1050 pixels; maximal luminance of 250 cd/m²; distance 0.5 m; dim office lighting conditions). Subjects were naïve with respect to the experiment, paid and with normal or corrected-to-normal vision. Each session took around 40 minutes. Please see the supplemental material for details.

In the first study, 9 subjects were presented two horizontally-aligned equidistant circular patches of the same random approximately-isoluminant colors (one with, chosen one without afterimages, randomized). They were located at a changing random position on the screen for a short period of time (200 ms). The subjects were asked to fixate a small cross at the screen's center. In every step, the brighter one of the two circles needed to be chosen by pressing "left" or "right". In 57.3 %, (std. dev. 2.5 %) of 2700 trials, the stimulus with afterimages was perceived brighter. While this result seems weak at first glance, it is important to notice that the setup of our study aims at eliminating a second bias. Towards the center of the screen, where the fixation point is located,

which projects on the fovea, brightness is perceived slightly stronger. Moving the patches to random locations eliminates this effect, but also reduces the measurable effect.

The second study aims at outlining the potential gain of perceived brightness when using afterimages. We relied on six subjects. This time, the patches were equidistant from the centerline of the screen, to avoid the fovea bias. The observer focused on the screen center and was asked to press "up" or "down" in order to adjust the randomly-initialized brightness of one patch to the brightness of the other, which used afterimages. The resulting factor was found to be statistically significant (1.83, std. dev. 0.23, involving 42 trials).

5. Discussion and Conclusion

In this paper, we simulated retinal processes to reproduce afterimages based on local bleaching of photoreceptors. Different from previous work using global bleaching statistics, we simulate local bleaching, as well as temporal, color and time-frequency behavior. We consider several other perceptual aspects to ensure a high fidelity and demonstrate the usefulness of our approach in a user study.

Without eye tracking, we have to assume a user fixating on the screen center, which is the main limitation in practice: A subject observing a complex HDR photo of a city at night on an LDR display would expect afterimages when looking around in the picture in an explorative fashion. However, afterimages only appear if the content changes e. g., camera movements or animations. Using eye tracking hardware to overcome this problem is exciting future work.

Our study shows that afterimages can create the impression of increased brightness, but it is not intended to be complete. More in-depth psycho-physical experiments, involving real stimuli such as light bulbs (e. g., to refine c_a and c_d) are left as future work. Similarly, an extensive study of the full parameter space (position, size, luminance etc.) would be of interest. We also cannot rule out that other related effects (motion sharpening, preference for brightness and colors, aesthetics) play a role. Finally, we plan to simulate other phenomena (e. g., glare), and to study the interplay of visual information for an improved viewing experience.

This work was partially funded by the Intel Visual Computing Institute at Saarland Univ. Thanks go to Sirko Straube for advice.

References

- [Ade82] ADELSON E.: The delayed rod afterimage. *Vision Research* 22, 10 (1982), 1313–18.
- [Alp71] ALPERN M.: Rhodopsin kinetics in the human eye. *J Physiol.* 217, 2 (1971), 447–471.
- [ARH78] ANSTIS S., ROGERS B., HENRY J.: Interactions between simultaneous contrast and coloured afterimages. *Vision Research* 18, 8 (1978), 899–911.
- [BBS09] BRATKOVA M., BOULOS S., SHIRLEY P.: oRGB: a practical opponent color space for computer graphics. *IEEE Computer Graphics and Applications* 29, 1 (2009), 42–55.

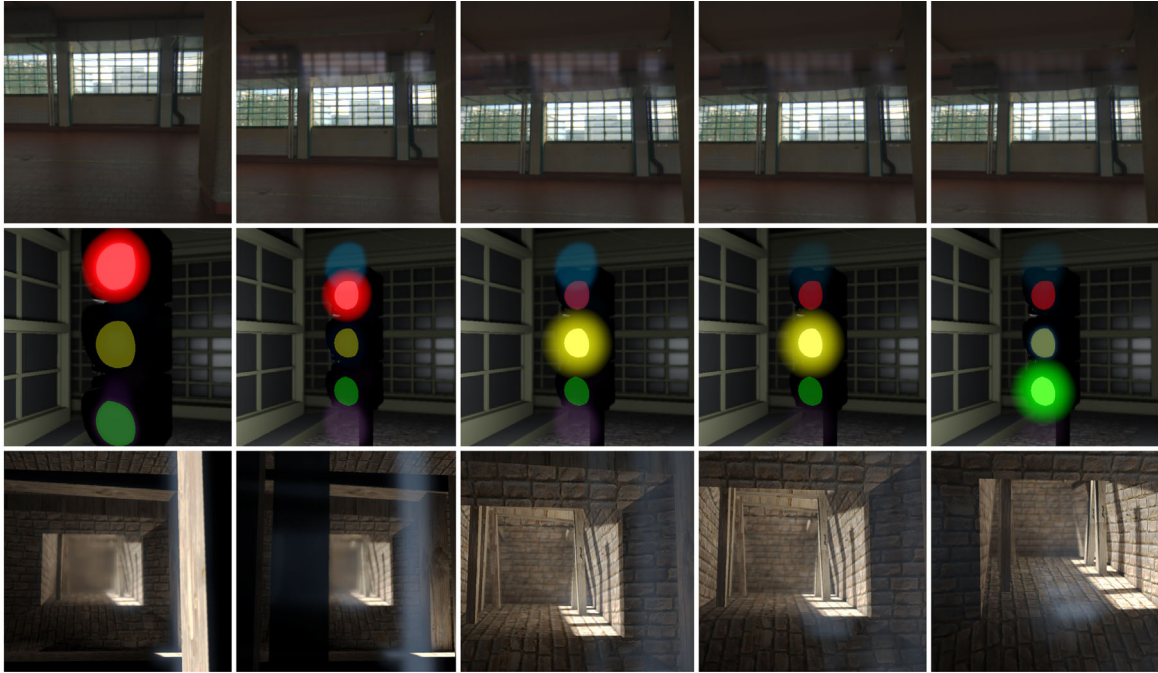


Figure 3: Video frames of an HDR image viewer (top), a traffic simulation (middle) and a game scenario (bottom) running in real-time. Please see the supplemental video for the animation. The strength is exaggerated for a better reproduction in print.

- [BHL74] BAYLOR D. A., HODGKIN A. L., LAMB T. D.: Reconstruction of the electrical responses of turtle cones to flashes and steps of light. *J Physiol.* 242, 3 (1974), 759–91.
- [Bri62] BRINDLEY G. S.: Two new properties of foveal after-images and a photochemical hypothesis to explain them. *J Physiol.* 164 (1962), 168–79.
- [Cre28] CREED R. S.: On the latency of negative after-images following stimulation of different areas of the retina. *J Physiol.* 66, 3 (1928), 281–98.
- [Dee05] DEERING M. F.: A photon accurate model of the human eye. *ACM Trans. Graph (Proc. SIGGRAPH)* 24, 3 (2005), 649.
- [Fai05] FAIRCHILD M. D.: *Color Appearance Models*, vol. 2nd. Addison Wesley Longman, Inc., 2005.
- [FJ04] FAIRCHILD M. D., JOHNSON G. M.: The iCAM Framework for Image Appearance, Image Differences, and Image Quality. *J Electronic Imaging* 13, 1 (2004), 1–34.
- [GAMS05] GUTIERREZ D., ANSON O., MUNOZ A., SERON F.: Perception-based rendering: Eyes wide bleached. In *Proc. Eurographics (Short Papers)* (2005).
- [HHDH09] HUBEL D. H., HOWE P. D. L., DUFFY A. M., HERNÁNDEZ A.: Scotopic foveal afterimages. *Perception* 38, 2 (2009), 313–6.
- [KJF07] KUANG J., JOHNSON G., FAIRCHILD M.: iCAM06: A refined image appearance model for HDR image rendering. *J Visual Communication and Image Representation* 18, 5 (2007), 406–414.
- [Lan64] LAND E. H.: The retinex. *Am Scientist* 52 (1964), 247–64.
- [Loo72] LOOMIS J. M.: The photopigment bleaching hypothesis of complementary after-images: a psychophysical test. *Vision Research* 12, 10 (1972), 1587–94.
- [LZL06] LU H., ZAVAGNO D., LIU Z.: The glare effect does not give rise to a longer-lasting afterimage. *Perception* 35, 5 (2006), 701–7.
- [MCMH04] MARTINEZ-CONDE S., MACKNIK S. L., HUBEL D. H.: The role of fixational eye movements in visual perception. *Nature reviews. Neuroscience* 5, 3 (2004), 229–40.
- [PCA*10] PAJAK D., CADIK M., AYDIN T. O., MYSZKOWSKI K., SEIDEL H.-P.: Visual maladaptation in contrast domain. In *Proc. SPIE* (2010), vol. 7527, pp. 752710–12.
- [PFFG98] PATTANAİK S. N., FERWERDA J. A., FAIRCHILD M. D., GREENBERG D. P.: A multiscale model of adaptation and spatial vision for realistic image display. In *Proc. SIGGRAPH* (1998), pp. 287–298.
- [PTYG00] PATTANAİK S. N., TUMBLIN J., YEE H., GREENBERG D. P.: Time-dependent visual adaptation for fast realistic image display. In *Proc. SIGGRAPH* (2000), pp. 47–54.
- [Rus65] RUSHTON W. A.: Bleached rhodopsin and visual adaptation. *J Physiol.* 181, 3 (Dec. 1965), 645–55.
- [SC33] STILES W. S., CRAWFORD B. H.: The Luminous Efficiency of Rays Entering the Eye Pupil at Different Points. *Proc. Roy. Soc. B* 123, 1 (1933).
- [Shu24] SHUEY A. M.: The Flight of Colors. *Am J Psych.* 35, 4 (1924), 559–579.
- [SKN01] SHIMOJO S., KAMITANI Y., NISHIDA S.: Afterimage of perceptually filled-in surface. *Science* 293, 5535 (Aug. 2001), 1677–80.
- [VCP80] VALLERGA S., COVACCI R., POTTALA E.: Artificial cone responses: A computer-driven hardware model. *Vision Research* 20, 5 (1980), 453–457.
- [VL77] VIRSU V., LAURIEN P.: Long-lasting afterimages caused by neural adaptation. *Vision Research* 17, 7 (1977), 853–860.